Egbert Keller*

On the unit cell volume expansion in homogeneous series of isotypic structures of "ionic" inorganic compounds

DOI 10.1515/zkri-2016-0005
Received January 26, 2016; accepted October 25, 2016

Abstract: Within a "homogeneous" series of (crystal-chemically) isotypic structures one and only one chemical element *E* of the sum formula is replaced successively by heavier elements of the same group of the periodic table. For corresponding series of "ionic" compounds, a (coarse) "expectation value" ΔV_{th} for the unit cell volume expansion following the replacement of *E*(*i*) by *E*(*j*) (with $i<j$ = row numbers in the periodic table) can be calculated by using the empirical formula $\Delta V_{th} = 56.5\ (z_E\ \Delta\rho_{E(i)\ E(j)}) - 0.80\ (z_E\ \Delta\rho_{E(i)\ E(j)})^2$, where z_E is the number of atoms *E* per unit cell and $\Delta\rho_{E(i)\ E(j)}$ is the linear statistical size (= radius) difference for the two elements *E*(*i*) and *E*(*j*). Two hundred and twenty-eight different series have contributed to the statistical evaluation of this formula. Series for which *E* are elements of low valence have been excluded *a priori* from the calculations if the residual atoms of higher valence by themselves form an infinite framework, as it was suspected, that in structures of this kind the "natural" volume expansion caused by the *E*(*i*) → *E*(*j*) size increase is hampered by the rigidity of this framework. Application of the above formula to structures of this kind clearly supports this suspicion only, if the framework is of dimensionality three. The results derived from all other investigated structures are qualitatively compatible with the "volume increments rule" published in the 1930s. This suggests that they should be applicable also to isotypic series of crystal structures defined in a less restricted manner.

Keywords: ICSD; isotypic structures; unit cell volume.

Introduction

Two structures are said to belong to the same "structure type" if they are *isoconfigurational*, meaning that they belong to the same space group type, that the complete sequences of the occupied Wyckoff positions are the same (after standardization of the structural data) and that positional parameters and coordinations of corresponding atoms are similar [1]. Pairs or groups of *isoconfigurational* structures can be found in the Inorganic Crystal Structure Database, ICSD [2, 3] due to the equipment of the structure entries with structure type information [4]: in the current version of the ICSD [3], about 140,000 of the more than 180,000 crystal structure entries have been assigned to more than 9000 different structure types.

Two *isoconfigurational* structures are classified *crystal-chemically isotypic*, if the varying atoms are similar from a chemical and physical point of view [1]. For the present work, in postulating that atoms of one group (column) of the periodic table generally are chemically/physically similar, we define a "*homogeneous* series *of (crystal-chemically) isotypic structures*" (HSIS) as a series of *isoconfigurational* structures where one (and only one) element *E* present in the sum formula varies within *one* group of the periodic table. In the present text, such a series will be written in the form

$$A_aB_b\ldots[E(i)E(j)\ \ldots]_e\ldots P_pQ_q$$

where *A*, *B*, *E*(*i*), *E*(*j*), *P*, *Q* represent element symbols, *a*, *b*, *e*, *p*, *q* are stoichiometric coefficients and $i<j$ denote period (row) numbers of the periodic table. For example, the homogeneous series Bi*OX* (*X* = F, Cl, Br, I) [5] is written as BiO[F Cl Br I].

In the text below, in most cases the common structure type (STT) and individual ICSD collection codes (ICC) of the series members (instead of literature references) will be indicated additionally. A series may contain gaps within the *E* sequence because the corresponding structures have not been determined or do not match certain quality criteria (see below). In the formula, any such gaps are represented by "*", e.g.: [Li Na K * Cs]$Zr_2P_3O_{12}$ (STT: $NaZr_2(PO_4)_3$; ICC: 201935, 467, 4427, 250172).

The "depth" *d* of a HSIS might be defined as the number of periods in the periodic system which is spanned by it, while its "order" *n* specifies the number of its members. Thus, the above Bi*OX* series is of depth *and* order 4, the *A*$Zr_2P_3O_{12}$ series, also being of order 4, is of depth 5.

***Corresponding author: Egbert Keller,** Kristallographie, Institut für Geo- und Umweltnaturwissenschaften, Albert-Ludwigs-Universität Freiburg i.Br., Hermann-Herder-Str. 5, 79104 Freiburg i.Br., Germany, E-mail: egbert.keller@krist.uni-freiburg.de

The structural differences between the members of a HSIS lead to some kind of "differential crystallography" as they allow to study how a crystal structure reacts in answer to a small perturbation, namely the slight "blow up" of its *E*(*i*) atoms when they are replaced by (usually larger) *E*(*j*) atoms further down in the periodic table, while all other atoms, the connection scheme, and the translational periodicity remain the same. The study of such differences has led, for example, to insights into atomic interactions which the look at one of the structures alone could not have offered [5–7].

Structural differences within a HSIS can be visualized by superimposing images of the different structures, drawn with a common scale factor and aligned the same way, such that corresponding positions, e.g. the unit cell centers, coincide (see, for example, [5–7] and the structure representations in this article).

As can easily be seen from such superimpositions, a common feature of almost all HSIS is an increase in unit cell volume when *E*(*i*) is replaced by *E*(*j*). The reason is that the atoms coordinated to *E* are shifted away from the *E* positions according to the linear size (radius) difference Δr between *E*(*i*) and *E*(*j*) (Figure 1).

The growing of the unit cell volume with increasing size of *E* seems to be trite. However, the question, by which amount ΔV the volume will grow, if the *E*(*i*)- (but not the *E*(*j*)-) structure volume is known, is less trivial. Of course, *in praxi*, the answer could simply be obtained quantitatively by a powder diffractogram, but the results would certainly not provide for any *general* insights. With the work presented here we tried to find some *principles* which play a role in determining ΔV within the *average* HSIS of "ionic" compounds. Such efforts might be classified *art pour l'art*, but we nevertheless thought it worthwhile to have an analytical look at a phenomenon which can be observed in thousands of special well-defined series of crystal structures.

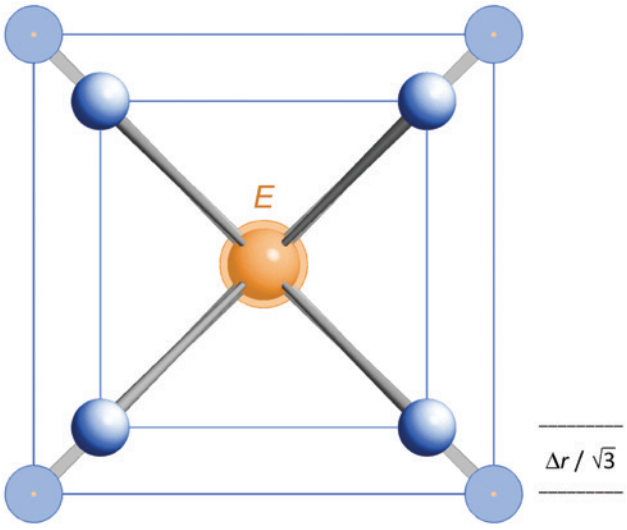

Fig. 1: Unit cell volume expansion for a structure *EX* belonging to the CsCl structure type. In the transition *E*(*i*) → *E*(*j*), *E*–*X* bond lengths grow by Δr. The *E*(*i*) [*E*(*j*)] structure has been drawn by solid 3D [flat] shading.

Preliminary mechanistic considerations

For simple structure types, the above question concerning ΔV can be answered rather precisely: In Figure 1, for example, the volume growth in the transition *E*(*i*) → *E*(*j*) is visualized for a simple *EX* structure belonging to the CsCl structure type. The *X* atoms at the unit cell corners are shifted by Δr in the <111> directions, and the volume *V*(*j*) of the *E*(*j*) unit cell can be calculated from the edge length *a* of the *E*(*i*) cell and Δr according to (1) (with $t = 2/\sqrt{3}$):

$$V(j) = (a + t\Delta r)^3 = a^3 + 3a^2\ t\Delta r + 3a\ (t\Delta r)^2 + (t\Delta r)^3 \\ = V(i) + 3a^2\ t\Delta r + 3a\ t^2\Delta r^2 + t^3\Delta r^3 \quad (1)$$

In neglecting the Δr^3 term ($t\Delta r << a$), the volume increase ΔV is approximately given by (2):

$$\Delta V \approx 3t\ (a^2\Delta r + t\ a\ \Delta r^2) = 3t\ (V(i)^{2/3}\Delta r + t\ V(i)^{1/3}\Delta r^2) \quad (2)$$

Obviously, ΔV increases with increasing Δr *and* with increasing *V*(*i*) in different non-linear manners. If *E* and its coordination polyhedron are embedded into a larger structure, the Δr shifts are supposed to propagate into regions further away from *E* inasmuch as the shifted atoms try to retain the distances to the other atoms, to which they are also coordinated. In principle, such an expansion "wave" might propagate outwards until the border faces of the unit cell are reached (while some distortions in the outer regions will become necessary, to retain translational symmetry). This naïve "expansion model" is visualized in Figure 2 for two virtual, made-up structures exhibiting fragments with CsCl structure in the centers of the unit cells. As the atoms in the unit cell corners are also shifted by Δr in the <111> directions, the model implies, that the edge length *a* of the *E*(*i*) unit cell also grows by $t\Delta r$, meaning that (2) would also be applicable here. However, at equal Δr values, the resulting ΔV should be much larger this time, as *V*(*i*) is much larger than in the *EX* case above. It should be noted, by the way, that *t* would adopt other values, for example 2, if the bonds from *E* to its neighbors were directed differently, for example parallel to <100> (instead of to <111>).

Now, even if the simple expansion model underlying Figure 2 was generally valid in principle, (2) would

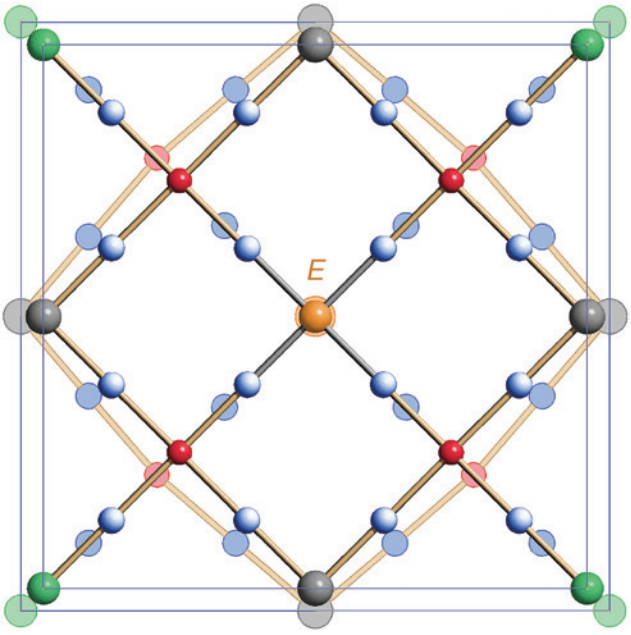

Fig. 2: A possible expansion model for a made-up structure with *Pm*3*m* symmetry and $a = 12$ Å in the transition $E(i) \rightarrow E(j)$. All bond sticks are directed (approx.) parallel to <111>. A Δr of 0.87 Å has been assumed, meaning that the bond lengths to $E(i)$ and all halves of the unit cell space diagonals grow by this amount, such that a for the larger cell is 13 Å.

certainly not be applicable generally, if only because most cases do not belong to the cubic system. But at the beginning of this investigation it seemed at least reasonable to assume, that the volume expansion ΔV for an $E(i) \rightarrow E(j)$ transition is generally dependent from the initial volume $V(i)$ and the linear E size difference Δr (but see section "Comparison with results derivable from Biltz' volume increments rule", below). Furthermore, a third quantity was considered to play an important role in this respect: The E concentration, $c_E = z_E/V(i)$ (with z_E = number of E atoms per unit cell): the pressure for the unit cell to expand certainly increases the more atoms E per given volume are "blown up". To find out how ΔV is generally (i.e. per average) related to these three quantities, a statistical analysis of volume difference data provided by numerous HSIS retrieved from the ICSD has been performed.

Experimental

Computer programs

The computer program FINDIS was used to find and retrieve HSIS from the ICSD (for a short note on FINDIS, see [8]). As an input, FINDIS requires an ASCII file consisting of ICSD entries in the "long-view" format. The entries are not required to include any atomic parameter information. The present work bases on a corresponding ASCII file [9] representing the complete ICSD (minus atomic parameters) in its 2013/2 state. This ICSD version had more than 160,000 entries, the majority of them assigned to more than 6000 structure types.

HSIS to be found by FINDIS can be filtered due to a number of criteria like structure type, minimal series depth d (with/without gaps allowed), measurement temperature/pressure and max. R value (of the series members). It should be noted, that certain types of structures or series can principally not be recognized by FINDIS: (a) structures with non-integer coefficients in the sum formula, (b) HSIS composed of members with a different number of atoms per unit cell (e.g. the structures of NH_4Cl and NaCl).[1]

To explain, why in the present text, e.g. a certain ICSD collection code (ICC) appears behind a series formula (and not that one of another entry of the same structure), or why the design of some of the series formulas is unconventional, some FINDIS process steps, are briefly described in the following. For example, at program start, FINDIS automatically extracts all the different structure type names from the ASCII file and stores them in a table in alphabetical order. In searching for HSIS, the following procedure is then usually performed for each structure type name stored in the table:

The ASCII file is searched for all structure entries which contain the structure type name in question in the corresponding record and match the optionally set filter criteria. If a certain structure is present in more than one entries, that one with the lowest R value indicated is chosen. If two or more entries exhibit the same R value, the one with the most recent publication year is selected. All other entries (of the same structure) are discarded. HSIS are then found by comparing the sum formulas of all remaining entries (one per compound). To this end, all formulas are reduced to the corresponding "root formulas" with all coefficients coprimes, while Z (the number of formula units per unit cell) is increased correspondingly. Furthermore, it is necessary for comparison, that the different components in all sum formulas are ordered the same way. This is done according to the pattern in the sum formula of the first entry in the list (meaning that in few cases the resulting order of the elements is a bit unusual). Subsets of all formulas are then sought which differ only at one element position E. From any of such subsets all smaller subsets are sought within which this position is occupied exclusively by elements of one periodic table group. The structures belonging to any of these smaller subsets form a new HSIS.

The series formula is then constructed and output by the program. Optionally, the program adds data like ICCs, publication years, R values, z_E and unit cell parameters including volumes, furthermore parameter differences for the pairs of "vicinal" structures, with $E(i)$ and $E(j)$ being direct neighbors in the series formula.

FINDIS output files can be re-sorted and/or filtered by some additional programs. E.g. the output can be filtered by means of the program TABLIS with respect to desired ranges of parameters like periodic table position of $E(i)$, $V(i)$, ΔV_{ex}, z_E, c_E, and $\Delta\rho_{E(i)\,E(j)}$. The latter are – or base on – statistically determined tabulated Δr values for $E(i)/E(i+1)$ pairs [10]. For two elements not directly vicinal in the corresponding periodic table group, the $\Delta\rho_{E(i)\,E(j)}$ value is determined by summing up the appropriate tabulated values. For example, $\Delta\rho_{Na\,Cs}$ is estimated by calculating the sum $\Delta\rho_{Na\,K} + \Delta\rho_{K\,Rb} + \Delta\rho_{Rb\,Cs}$, the result (0.60(5) Å) matching the value determined by a subsequent direct RADDIF [10] comparison of Na and Cs (0.60(5) Å). In all cases

1 This restriction does not pertain to cases, where some series members have been described in a rhombohedral and others in a hexagonal setting.

relevant for the calculations described below, except four [one (Co → Ir)], the two values differ by ≤ 0.01 [0.02] Å (or ≤ 4 [6] %). TABLIS calculates ΔV_{th}, $Q_{\Delta V}$ and $D_{\Delta V}$ values (see below) for *all* pairs of structures in a series and performs statistical calculations if more than one series is processed.

In order to visualize and compare crystal structures and generate the corresponding illustrations for this article, the program SCHAKAL [11] has been used. To save space, all HSIS chosen to be illustrated belong to the cubic system (implying that one axial projection of the unit cells is sufficient for visualization). The mathematical diagrams in this article were generated by means of the program Origin [12].

Generating a subset of all retrievable HSIS

With indicated measurement temperatures (if any) restricted to the range 248–348 K and with indicated measurement pressures (if any) below 10 kPa, and with no other filters active, a search of the 2013/2 ICSD file by FINDIS yields 12,468 HSIS of depth 2–6 (gaps allowed) belonging to 2510 different structure types.

All members of the HSIS to be used for the statistical analysis of unit cell volume expansion were visually checked beforehand for isotypism (see below), actually a time-consuming task. Therefore, the number of 12,468 HSIS was substantially reduced to a practicable amount by the following formal measures:

1. The series to be retrieved by FINDIS were restricted to those of depth ≥ 3 (gaps allowed) with all member structures equipped with an indicated *R* value ≤ 0.15. By these two restrictions alone the number of retrieved series shrinks to 1120 belonging to 512 different structure types.
2. From the remaining list, series or structures were "manually" excluded if they (or the corresponding compounds) fulfilled at least one of the following criteria/properties (some with few exceptions): (a) metals or alloys, (b) compounds with unusual valences of *E*, like carbonyls, suboxides etc., (c) *E* belonging to transition metal columns three (because of the complication caused by lanthanides and actinides), eight (because of a probably too small $\Delta\rho_{Fe\,Ru}$ value of 0.01(2) Å) and 11 (because of $\sigma > 0.05$ Å for $\Delta\rho_{Ag\,Au}$), (d) disorder reported for some or all member structures, (e) all structures of the series determined by Rietveld analysis (except for very simple structures or when all contributing structures have been published in one article.
3. Of the remaining series almost all were taken for which the structures have unit cell volumes > 700 Å^3, as series with this property turned out to be comparatively rare. From the rest about 50% were randomly selected.

From the finally selected series, those failing in the isotypism test (see below), were rejected. Two hundred and ninety-one series, belonging to 229 different structure types, survived the whole procedure. Some of the remaining structure types and the corresponding series (with *E* = alkali or halogen) were additionally excluded *a priori* from the general statistical analysis by a *non-formal*, i.e. problem-related, criterion which is further explained in section "Series of structures …", below. Eventually, 228 series remained, belonging to 170 different structure types. The 228 series contain 569 pairs of isotypic structures. Pairs with $\Delta V_{ex} \leq 0$ or with $\Delta\rho \leq 0$ were additionally excluded from the statistical analysis for mathematical reasons, thus reducing the latter number to 557.

Tests for isotypism

HSIS surviving the exclusion procedure described above were checked for the isotypism of all members. This was done visually, using SCHAKAL [11] scripts which allow the automatic side-by-side generation of images of a structure model as seen from three different directions on one screen. Initially, isotypism checks were done because of a misinterpretation of the term *isoconfigurational* which had been mixed up by the author with the term *isopointal*. The mistake was realized, when at some point almost all checked series had turned out to consist of isotypic members only. But checking was nevertheless continued, as few examples of non-isotypism (at least in a meaning relevant for this study) had actually been found meanwhile. The cases that finally led to an exclusion from the HSIS pool are described in the following, as they are considered to be of interest beyond the issue of this work:

In the two series [*Li* * * * Cs]UNbO$_6$ (STT: KUO$_2$VO$_4$; ICC: 416590, 60945) and [K Rb *Cs*]$_2$GaSb$_2$ (STT: K$_2$GaSb$_2$; ICC: 53579, 300135, 300156) the members for which *E* is printed in italics apparently do not belong to the indicated structure type. Other cases were found, where isotypism might be stated in general but the similarity of the structures was not judged sufficient for the intentions of the present study. For example, in the series [Na K Rb Cs]$_3$Fe$_2$S$_4$ (STT: Na$_3$Fe$_2$S$_4$; ICC: 100357, 79224, 79225, 79226), the structure and alignment of the $\{^1_\infty\}Fe_2S_4^{3-}$ rods in the Cs member differs from the ones in the other three members, thus leading to a substantially differing coordination polyhedron for Cs. In the series [K Rb Cs]AsOF$_4$ (STT: K$_2$As$_2$F$_8$O$_2$; ICC: 9027, 9028, 6070), the translation lattice of the Cs structure is shaped rather differently: β becomes approx. 105° (to be compared with 92° and 92°) when the structure is described – like the K and Rb structures – with space group $P2_1/n$ instead of $P2_1/c$. Finally, in some series *E*(*i*) and *E*(*j*) play different roles (i.e. occupy different positions) in the different structures. This pertains to the series KGe[P * Sb]O$_5$ (STT: KTiPO$_5$; ICC: 39735, 39463), [Mg Ca Sr]$_3$Y$_2$Ge$_3$O$_{12}$ (STT: Al$_2$Ca$_3$Si$_3$O$_{12}$; ICC: 280049, 280048, 80582), and – for obvious reasons – [Na * Rb]KS, [Li * * Rb]NaS and As[P * Sb]O$_5$. All these series have either been excluded from the statistical analysis or the differing member has been removed from the series.

Results and discussion

Statistical analysis

Aim of the statistical analysis of the finally remaining 228 HSIS was to find a function $\Delta V_{th} = f(\Delta r, V(i), c_E)$ (see end of section "Preliminary considerations…", above) and to test the quality of *f* by comparing the ΔV_{th} values calculated by it to the corresponding experimental values ΔV_{ex} for all HSIS in the pool. As already mentioned, $\Delta\rho_{E(i)\,E(j)}$ values [10] were used as linear size differences Δr.

To get an idea on how, for example, $V(i)$ influences ΔV, the data of the 233 series were filtered for a narrow range of c_E (say, 0.002–0.006 Å^{-3}) and a narrow range of $\Delta\rho_{E(i)\,E(j)}$ (say, 0.32–0.34 Å). Then the ΔV_{ex} values of this subset were drawn as a function of $V(i)$. This was done for different

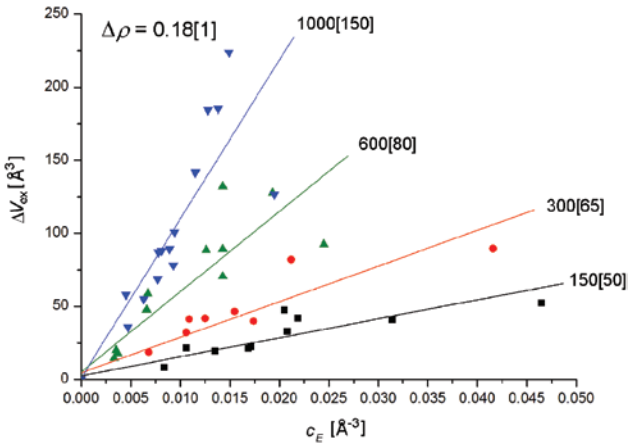

Fig. 3: ΔV_{ex} as a function of c_E for pairs of isotypic structures with $\Delta\rho_{E(i)\,E(j)}$ values of 0.18 ± 0.01 Å. Different subsets belonging to different $V(i)$ ranges (e.g. 150 ± 50 Å³, denoted as 150[50]) are represented by symbols of different shape and color. For each subset the corresponding least-squares line is shown.

c_E and $\Delta\rho_{E(i)\,(Ej)}$ ranges. In corresponding manners, plots of ΔV_{ex} vs. c_E (Figure 3) or vs. $\Delta\rho_{E(i)\,E(j)}$ were generated.

The diagrams suggested unexpectedly, that ΔV_{th} simply is approx. proportional with respect to *all* three variables, thus leading to (3) (with p' = a constant [Å²] and $c_E = z_E/V(i)$ [Å^{-3}]). After reduction, and other than expected from (2), (3) lacks any dependence from the initial volume $V(i)$.

$$\Delta V_{th} \approx p'V(i)\; c_E \Delta\rho_{E(i)\,E(j)} = p' z_E\; \Delta\rho_{E(i)\,E(j)} \qquad (3)$$

The parameter p' was adjusted such that the mean value for all the quotients $Q_{\Delta V} = \Delta V_{ex}/\Delta V_{th}$ became 1, or, to be more precise, that the mean value for all $\log_{10}(Q_{\Delta V}) = \lg(Q_{\Delta V})$ values became 0. Logarithmic values of the quotients are used here, as their value ranges spread symmetrically about the (ideal) mean value 0, while this is not true for the $Q_{\Delta V}$ values themselves [which principally cover the small range 0–1 on the lower side, but the large range 1 to ∞ on the upper side of the (ideal) mean value 1].

If p' was set to 54.5 Å², $<\lg(Q_{\Delta V})> = \sum_1^m [\lg(Q_{\Delta V})]/m$ for the $m = 553$ (four extreme outliers excluded, see below) structure pairs actually became 0.000(152), thus (3) can be replaced by (4):

$$\Delta V_{th} = 54.5\, z_E\; \Delta\rho_{E(i)\,E(j)} \qquad (4)$$

$<Q_{\Delta V}>$, the average of all $Q_{\Delta V}$ values is 1.06(38) and $<D_{\Delta V}>$, the average of all differences $D_{\Delta V} = \Delta V_{ex} - \Delta V_{th}$, is – 9(68) Å³. An R-value calculated similarly as for structure analyses ($R = \sum_1^m |<Q_{\Delta V}> - Q_{\Delta V}| / \sum_1^m <Q_{\Delta V}>$) resulted in 0.26.

In Figure 4a, ΔV_{ex} is plotted against z_E for different narrow ranges of $\Delta\rho_{E(i)\,E(j)}$, the straight lines visualize (4)

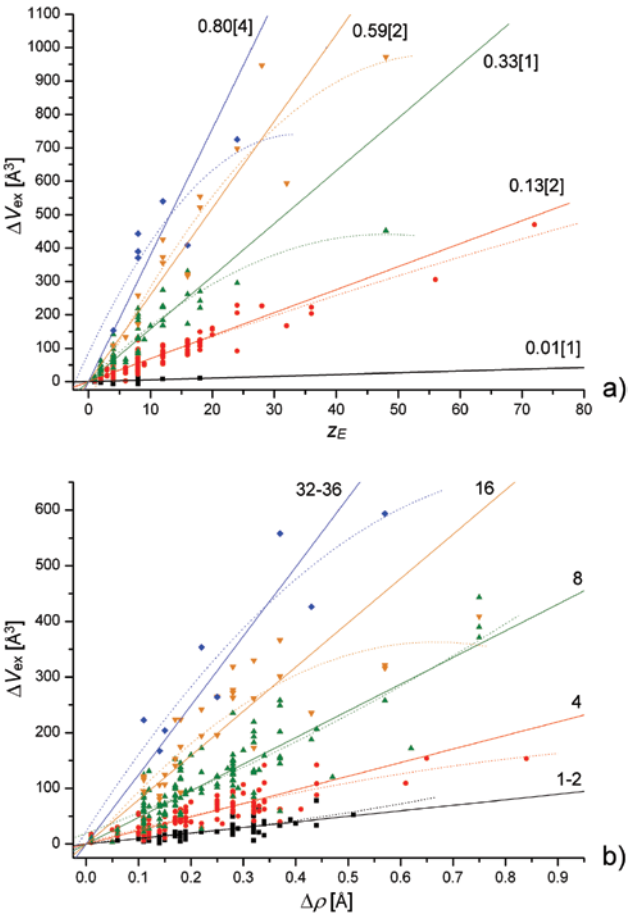

Fig. 4: ΔV_{ex} as a function of z_E (a) and $\Delta\rho$ (b) for different values or ranges of $\Delta\rho$ (a) and z_E (b). For the different straight lines and parables, see text. For the meaning of the square brackets, see caption of Figure 3.

for the different mean values of the $\Delta\rho_{E(i)\,E(j)}$ ranges. Similarly, in Figure 4b, ΔV_{ex} values are plotted against $\Delta\rho_{E(i)\,E(j)}$ for different values or ranges of z_E.

Despite the relatively severe scattering, the principal validity of (4) can be seen from the two diagrams. Parables fitted to the different data groups in Figure 4 (dotted lines) reveal, however, that ΔV_{ex} is overestimated per average for larger z_E *and* larger $\Delta\rho_{E(i)\,E(j)}$ values. This can be compensated by adding a quadratic term to (3) as shown in (5):

$$\Delta V_{th} = p\, z_E\; \Delta\rho_{E(i)\,E(j)} - q\; (z_E\; \Delta\rho_{E(i)\,E(j)})^2 \qquad (5)$$

p [Å²] and q [Å] were adjusted, such that both, $<\lg(Q_{\Delta V})>$ and $<D_{\Delta V}>$, became zero: $<\lg(Q_{\Delta V})> = 0.000(148)$, $<D_{\Delta V}> = 0(45)$ Å³. The corresponding parameter values are given in (6). The "R-value" resulted in 0.25, i.e. less than for (4), just as $|<D_{\Delta V}>|$ and the σ values of $<\lg(Q_{\Delta V})>$ and $<D_{\Delta V}>$.

All calculations were performed with unit weights.

$$\Delta V_{th} = 56.5\, z_E\, \Delta\rho_{E(i)\,E(j)} - 0.80\, (z_E\, \Delta\rho_{E(i)\,E(j)})^2 \quad (6)$$

The series contributing to the statistical analysis are listed in Table 1. Figure 5 shows the distribution of the $\lg(Q_{\Delta V})$ values for all 557 data points. The figure resembles a normal distribution, the above σ value of 0.148 means that the quotients $\Delta V_{ex}/\Delta V_{th}$ vary from 0.7 to 1.4 within the 1σ range and from 0.5 to 2.0 in the 2σ range. Thus, calculated ΔV values should be "reliable" in the limits of 50–200%.

In Figure 6, the ΔV_{ex} values of the data set are plotted against the corresponding ΔV_{th} values. Ideally, the data points should occupy the straight line of slope 1, $\Delta V_{ex} = \Delta V_{th}$ [i.e. $\lg(Q_{\Delta V}) = 0$], the 1σ and 2σ regions of $<\lg(Q_{\Delta V})>$ are shaded with decreasing intensity. The considerable scattering of the data points can partially be assigned to uncertainties in the $\Delta\rho_{E(i)\,E(j)}$ values, the standard deviations of which are mostly in the range 0.01–0.04 Å [10]. Thus, for smaller $\Delta\rho_{E(i)\,E(j)}$ values, σ may amount to 25% or even more [e.g. $\Delta\rho_{K\,Rb} = 0.11(3)$ Å]. Correspondingly, the largest scattering (in terms of σ) occurs in the leftmost part of Figure 6 where the contribution of structure pairs with small $\Delta\rho_{E(i)\,E(j)}$ values is comparatively large.[2] Except from this (and possible experimental data errors), the scattering should mainly mirror the variety of individual solutions all the different structure geometries had to find in order to solve the problem of volume expansion with concurrent retainment of the bond connectivity scheme *and* of translational symmetry.

The different $\lg(Q_{\Delta V})$ values (= y), when plotted against $V(i)$ (= x) generate the least-squares line $y = 0$ (diagram not shown here). Thus, a general dependence of ΔV from $V(i)$ can actually be excluded.

In the range $\Delta V_{th} < 325$ Å^3 ($z_E\, \Delta\rho_{E(i)\,E(j)} < 6$ Å), values calculated by (4) and (6) differ by ≤ 5%, such that (4) can replace (6) if $z_E\, \Delta\rho_{E(i)\,E(j)} < 6$ (or even some more) Å. For the 512 structure pairs (93% of all) falling into that range (4) corresponds to a $<\lg(Q_{\Delta V})>$ of 0.005(154) and a $<D_{\Delta V}>$ of −1(39) Å^3, with $R = 0.26$.

Dependence of $<\lg(Q\Delta_V)>$ from *E*

Another reason for the significant scattering of the data points in Figure 6 could also be, in principle, that different *E* elements behave differently with respect to volume expansion. Subsets of the HSIS pool were therefore formed within which only one kind of $E(i)$ (of a certain valence) is replaced by (different) $E(j)$. Table 2 lists the $<\lg(Q_{\Delta V})>_E$ values in the cases where the number *m* of contributing structure pairs exceeded 10. They run from −0.09(15) to 0.07(10) and seem to be distributed more or less randomly. Especially, there is no relationship between $<\lg(Q_{\Delta V})>$ and the valence of *E*, or its ionic radius (I.R.) (usually seen as a measure for atomic size). For example, the three mostly negative $<\lg(Q_{\Delta V})>_E$ values (−0.09 to −0.07) are produced by $Si^{+\,IV}$ (I.R. = 0.4 Å), $Sr^{+\,II}$ (1.4 Å) and $S^{-\,II}$ (1.7 Å).

If ΔV_{th} values belonging to the different elements are multiplied beforehand with the corresponding $10^{<\lg(Q)>}$ values (Table 2) in an analysis of *all* data, a $<\lg(Q_{\Delta V})>$ [$<\Delta D>$] of 0.006(139) [4(47) Å^3] is obtained (cf. the above 0.000(148) [0(45) Å^3]). Comparison of the two σ pairs suggests that the distinction between different *E* elements in the calculation of ΔV_{th} would mainly be an unnecessary complication.

In neglecting the small $<\lg(Q_{\Delta V})>_E$ differences in Table 2 we can finally state from (6) that an atom of *any* element *E* should, regardless of its properties, cause – per average – just the same ΔV, if only $\Delta\rho$ is the same.

Subsequent mechanistic considerations

Other than suggested by Figures 1 and 2 and by (2), ΔV_{th} is, as stated above, independent from the initial unit cell volume $V(i)$. (6) says, that for $\Delta r = 0.87$ Å (cf. Figure 2) one single $E(j)$ atom introduces (per average) a unit cell volume increase of 48.5 Å^3. For the virtual structure model of Figure 2 with $z_E = 1$ a "ΔV_{ex}" value of 469 Å^3 can be calculated. Thus, with $Q_{\Delta V} = 9.7$, this made-up structure pair would produce an *extreme* outlier with respect to (6). Obviously, the expansion model in Figure 2 is not realistic. Unfortunately, it was not possible to find a suitable real example with $z_E = 1$ (as in Figure 2) for comparison. Therefore the end members of the series $Be_3Mn_4Si_3[S\ Se\ Te]O_{12}$ ("HS-1") (STT: sodalite-frame; $z_E = 2$), will be used as a next-best example (Figure 7; $\Delta V_{ex} = 39.5$ Å^3):

Clearly, the Mn atoms in Figure 7, bonded to E = S in the center are shifted away from *E* in the <111> directions, when S is replaced by Te (S–Mn = 2.41, Te–Mn = 2.74 Å). As expected, the shift amount of 0.335 Å is close to $\Delta\rho_{S\,Se} + \Delta\rho_{Se\,Te}$ = 0.34 Å (for E^{-II}). Also the three O atoms bonded to Mn (2nd coordination sphere to *E*) are shifted outwards (the O atom labeled O' is shifted towards the viewer). But the shift directions are <311> instead of <111> and the shift magnitude is only 0.21 Å. The other metal ions coordinated to O (Be and Si, 3rd CS to *E*) are moved by 0.11 Å parallel <2 1 0>, implying 0.10 Å shifts in the <100> directions. And twice that amount makes just the increase of *a* in the transition S → Te ($\Delta a = 0.19$ Å). Meaning, that the 8 *E* atoms in the corners of the unit cell are shifted by only $1/2 \times 0.19 \times \sqrt{3} = 0.165$ Å outwards in the <111> directions,

Tab. 1: Structure types, ICSD Collection Codes, and Q (= $Q_{\Delta V}$) ranges for the HSIS contributing to Figures 5 and 6.

Structure type	Series formula	ICSD Coll. Codes			Q range
Ag3CsS2	K Cu3 [S * Te]2	100001	100830		0.88
Al2(SO4)3	[Al Ga In]2 S3 O12	73249	79304	79303	0.89–1.59
Al2Ca3Si3O12	[Mg Ca Sr]3 Y2 Ge3 O12	280049	280048	80582	0.73–0.84
	Li3 Na3 [Al * In]2 F12	9923	416929		1.24
Al2MgO4	Cr2 [Zn Cd Hg] Se4	626745	39416	402408	0.93–1.11[a]
	Zn [Al * In]2 S4	35380	81811		0.92
	Cr2 Hg [O S Se]4	245275	53129	402408	0.68–0.78
Al2O3	[Al Ga In]2 O3	92629	27431	16086	0.72–0.84
AlCe	K2 Cu [P As]	61082	43936		1.36
AlH2P3O10	[Al Ga In] H2 P3 O10	20857	39444	250399	1.47–1.58
AlPO4	[B Al Ga] P O4	413435	9641	33252	0.98–1.22
Ba(SCN)2	[Ca Sr Ba] C2 N2 S2	412783	94427	94428	1.43–1.46
Ba2MnS3	Ba2 Mn [S Se Te]3	26231	26230	1151	0.90–1.08
	Rb2 Ag [Cl Br I]3	280031	150287	150290	0.94–1.20
Ba4OCl6	[Ca Sr Ba]4 O Cl6	33883	402497	408175	1.04–1.07
	Sm4 O [Cl Br I]6	65166	416400	171016	0.78–0.87
BaBPO5	[Ca Sr Ba] B P O5	77518	97675	95116	0.77–1.05
BaCu2S2	Ba Cu2 [S Se Te]2	89573	89574	51444	0.78–0.89
BaMgSiO4	Na [B * Ga] Si O4	39459	411328		0.94
BaNiO3	Cs Mg [Cl Br I]3	22086	87260	87262	0.86–1.11
BaSO4	[K Rb Cs] Mn O4	89506	89507	89508	1.19–1.20
BaTiSi3O9	Ba [Ti * Hf] Si3 O9	18100	183835		1.99
BaZn2P2	Ba Mn2 [P As]2	10469	41794		1.06
Be2SiO4	Li2 [Cr Mo W] O4	1972	94489	15395	0.90–1.04
Bi4Te4(AlCl4)4	Al Bi [S Se Te] Cl4	414154	414155	411714	1.15–1.25
BiI3	[As Sb Bi] I3	23003	26082	78791	0.55–0.87[a]
Botallackite	Cu2 H3 O3 [Cl Br I]	153707	27493	27494	0.73–0.75
C60K6	[K Rb Cs] C10	66879	66880	657337	0.81–0.91
Ca2MgSi2O7	[Ca Sr Ba]2 Zn Ge2 O7	69387	39159	420550	0.72–0.84
Ca3Al2(OH)12	[Ca Sr Ba]3 Al2 H12 O12	202315	20529	26195	0.28–1.19
Ca3PI3	La3 [P As] I3	411801	411803		1.38
Ca5(PO4)3Cl	[Ca * Ba]5 P3 O12 F	99363	10029		0.91
CaCO3(hR10)	[Al * In] B O3	30538	75254		0.89
CaCO3(oP20)	[Ca Sr Ba] C O3	52152	202793	158378	0.93–1.09
CaFe2O4	Na Sc [Ti * Hf] O4	22208	22212		1.20
	Ba Lu2 [S Se Te]4	422891	422892	422893	0.76–0.97
CaMg(SiO3)2	Na [Al Ga In] Si2 O6	157730	156699	68741	1.09–1.11
CaWO4	[Na K Rb] Re O4	78831	1921	52339	0.93–1.62
CdI2	Ti [S Se Te]2	91579	108739	30051	0.53–0.64
Co(H2O)6SiF6	Co H12 [Si * Sn] O6 F6	2900	75984		1.96
Co2P2O7	Na [Al * In] P2 O7	400462	157157		1.34
CoSb2	[Co Rh Ir] P2	38316	174221	174222	0.91–1.15
Cr(NH3)5ClPtCl4	Mo [Co Rh Ir] H15 N5 O4 Cl	422144	169805	182290	0.76–1.28[a]
Cr3S4	V3 [S Se Te]4	79969	84195	52510	0.60–0.62
CrOOH(oP8)	[Al Ga In] H O2	91944	420004	15082	0.72–0.98
Cs2Au2Cl6	Cs Au [Cl Br I]3	6061	186067	186066	0.80–0.97
Cs2B12Cl12	Cs B6 [Cl Br I]6	151975	151976	151977	0.91–1.20
Cs2CuCl4	[K Rb Cs]2 Be F4	86154	61800	23152	0.92–1.31
	[K Rb Cs]2 Zn Cl4	80861	37070	6062	1.04–1.17
	Cs2 [Zn Cd Hg] Br4	69139	100592	54045	1.36–1.69
	Cs2 Zn [Cl Br I]4	6062	69139	82932	0.95–1.28
Cs2Pt(CN)4H2O2	[K Rb Cs]2 Pt H2 C4 N4 O2	418913	418912	418911	0.91–1.00
Cs2Pt3S4	Cs2 [Ni Pd Pt]3 Se4	33891	33892	33893	0.77–1.14
Cs2Zn3S4	Cs2 Mn3 [S Se Te]4	65253	78932	78933	0.93–1.24
Cs3CoCl5	Cs3 Mn [Cl * I]5	24	403102		1.20
Cs3Cr2Cl9	Cs3 [Cr Mo W]2 Cl9	94384	202290	202296	0.27

Tab. 1 (continued)

Structure type	Series formula			ICSD Coll. Codes	*Q* range
Cs3Cu2Cl5	Cs3 Cu2 [Cl Br I]5	150296	150297	65251	0.99–1.19
CsAu(N3)4	[K Rb Cs] Au N12	416489	416488	416487	1.51–1.53
CsCrBr3	Cs Cr [Cl Br I]3	10206	2590	8105	0.81–1.00
CsCu2Cl3	Rb Fe2 [S Se Te]3	99505	81547	81548	0.66–0.93
Cu2FeSnS4	Co Cu2 [Si Ge Sn] S4	99292	415927	99294	0.77–0.97
Cu2GeS3	Cu2 [Si Ge Sn] S3	88235	85138	91762	0.81–0.98
Cu3VS4	Nb Cu3 [S * Te]4	170784	169544		0.55
CuFeS2	Zn [Si Ge Sn] P2	23680	23706	648170	0.61–1.09
	Ag Ga [S * Te]2	23698	71007		0.90
Eu2CuS3	Cs2 Ag [Cl Br I]3	150286	150288	150291	1.06–1.20
EuGa2S4	Sr [Al Ga In]2 S4	46018	46019	300176	0.59–0.87
Faujasite-Fd3–frame	[Ca Sr Ba]23 Al46 Si50 O192	84463	88914	84464	0.23–1.02
FeBiO3	Cs Ge [Cl Br I]3	62557	62558	62559	0.72–0.95
FeF3	[Al Ga In] F3	68826	409507	38306	1.02–1.29
FeS2(cP12)	Ru [S Se Te]2	24186	68473	24188	0.56–0.57
	Os [S Se Te]2	300224	24202	300225	0.56–0.57
FeSe	Fe [S Se Te]	633302	169251	180602	0.57–0.70
FeZr6Cl14	Zr6 C [Cl * I]14	202915	60915		0.98
GaS	Ga [S Se Te]	201344	63122	43328	0.75–1.01
Gillespite	[Ca Sr Ba] Cr Si4 O10	30872	83464	83463	1.09–1.22
H3OAl3H14(PO4)8(H2O)4	[Al * In]3 H25 P8 O37	14141	152062		1.56
K2B12H12	[K Rb Cs] H6 B6	98616	98617	92501	1.68–2.02
K2C2O4H2O	[K Rb Cs]2 H2 C2 O5	246783	240494	249312	1.18–1.28
K2CuNbSe4	K2 [V Nb Ta] Ag S4	66840	84292	84294	0.95–1.88
	Cs2 [V Nb Ta] Ag S4	50460	84293	84296	1.75–2.59
K2GaSb2	[K Rb]2 Ga Sb2	53579	300135		1.19
K2GeF6	[K Rb Cs]2 Pt F6	87360	35108	35107	1.02–1.11
	H8 [Si * Sn] N2 F6	18027	409509		1.07
K2InCl5H2O	[K Rb Cs]2 In H2 O Cl5	200970	63007	63008	0.57–1.15
K2Mg(SO4)2(H2O)6(mP)	[K Rb Cs]2 Co H12 Se2 O14	409999	409720	409748	1.16–1.20
	[K Rb Cs]2 Zn H12 S2 O14	409985	409496	409742	1.11–1.22
K2MgF4	[Na K Rb]4 O Br2	67283	68505	411954	0.92–1.50
K2MnS2	K2 Zn [O * * Te]2	34603	420088		1.17
	Cs2 Mn [S Se Te]2	65455	65458	65461	0.96–1.48
K2NaAlF6	[Na K Rb] Cs2 Bi F6	9382	9383	9384	1.33–1.83
	Na [Al Ga In] H8 N2 F6	249157	418737	79099	1.13–1.65
	Na Cs2 Y [F Cl Br]6	25368	65732	65733	0.92–1.07
K2NaV5O14(H2O)5	Na [K * Cs]2 V5 H10 O19	413337	97737		0.98
K2P2S6	[K * Cs] P S3	33278	33277		1.37
K2Pb(SO4)2	[Ca Sr Ba]3 P2 O8	158736	150869	69450	0.73–0.76
K2PbCu(NO2)6	Cu [K * Cs]2 Pb N6 O12	26228	2381		0.85
K2PtCl4	[K * Cs]2 Pd Cl4	65036	95813		1.63
K2PtCl6	[K * Cs]2 Ta Cl6	59894	240711		0.70
	[K Rb Cs]2 Sn Cl6	1668	65059	9023	0.91–0.93
	W [K Rb Cs]2 Cl6	409840	409632	409674	0.81–1.17
	K2 [Mn Tc Re] Cl6	9679	22096	23769	1.96–2.25
	Cs2 Pt [F * * I]6	78955	201309		0.89
K2RuNOCl5	K2 Ru N O [Cl Br I]5	20436	68669	68670	0.96–1.07
K2S3	Cs2 [S Se Te]3	14094	14095	53244	0.84–1.10
K2SO4(beta)	[K Rb Cs]2 Ru O4	415749	415748	33799	0.94–1.27
K2SrCu2(NO2)6	K2 [Ca Sr Ba] Cu N6 O12	6183	178	1830	1.45–2.18
K2Zn(CN)4	K2 [Zn Cd Hg] C4 N4	14368	168524	62084	1.11–1.81
K3AlSe3	[K * Cs]3 Al Te3	300168	300181		1.12
	K3 Ga [S Se Te]3	300169	300170	300171	1.03–1.35
K3BP2	[K Rb Cs]3 B As2	300105	402082	300122	1.02–1.13
K3BS3	[K Rb Cs]3 B S3	411607	411609	391170	0.84–1.50

Tab. 1 (continued)

Structure type	Series formula	ICSD Coll. Codes			*Q* range
K3IB12H12	[K Rb Cs]3 H12 B12 Br	414581	414583	414584	0.91–1.18
	Rb3 H12 B12 [Cl Br I]	414585	414583	98620	0.66–1.64
K3Pr2(NO3)9	[Na * Rb]3 Nd2 N9 O27	402784	86308		1.24
K3VO4	K Ag2 [P * Sb] S4	420033	82143		1.09
K4CdCl6	Na [Ca Sr Ba]3 Ru O6	50170	50023	405133	0.65–0.70
K4Nb2S11	[K Rb Cs]4 Ta2 S11	410671	59373	59374	1.03–1.23
K4Ni(N3)6(H2O)2	[K Rb Cs]4 Ni H4 N18 O2	100841	100842	100843	1.22–1.34
K4P6	[K Rb Cs]2 P3	33259	65184	65185	0.95–1.26
K5Sb3Sn	Na5 [Si Ge Sn] P3	60077	60078	300189	0.79–1.26
K6HgS4	Na6 Mn [O S Se Te]4	420410	65447	65449	1.02–1.43
		65451			
	K6 Mn [S Se Te]4	65448	65450	65452	1.28–1.57
	K6 Cd [O * * Te]4	62053	420087		1.39
K9Fe2S7	[K Rb]9 Fe2 S7	73053	73054		1.05
	K9 Fe2 [O S Se]7	174311	73053	73055	1.16–1.37
KAl(SO4)2(H2O)12	Cs [Co Rh Ir] H24 S2 O20	201214	30747	30748	1.32–1.91[a]
	Cs [Al Ga In] H24 S2 O20	14316	201216	201217	1.34–2.24
	Cs [Al * In] H24 Se2 O20	68908	68912		1.29
KBO2	[Na K Rb Cs] B O2	34645	16005	59826	0.79–1.18
		74888			
	[Na K Rb] B S2	79613	79614	79615	0.88–1.37
KInS2	K Ga [S Se Te]2	49546	423188	411170	0.93–1.34
KLi2(OH)3	Li2 [K Rb Cs] H3 O3	65148	65149	65150	1.02–1.13
KOH	[Na K Rb] H O	26833	61047	61048	0.57–1.02
KOs(NH3)6(ClO4)2Cl2	[K Rb Cs] Ru H18 N6 O8 Cl4	280489	280491	280494	1.94–2.11
KTiCl3	K Ti [Cl Br I]3	154259	154260	154261	0.75–0.85
La2O3	[Ca Sr Ba] Cd2 P2	100063	30912	30915	0.78–0.84
	Li2 Ce [N P As]2	34003	42016	32042	0.94–1.00
La3CuSiS7	La3 Cu [Si Ge Sn] S7	23519	95025	155936	0.37–0.92
	Ce3 Cu [Si Ge Sn] Se7	156282	154743	152824	0.65–0.77
LaF3(P63mc)	[Na * * Cs]3 As	81566	409668		0.99
Li2ZrF6	[Ca Sr Ba] Sb2 O6	74539	74540	74541	1.04–1.16
Li4PbO4	Li4 [Ge * Pb] O4	65177	38350		0.78
Li6SrLa2Bi2O12	Li6 [Ca * Ba] La2 Ta2 O12	163860	163861		0.93
Li7TaN4	Li7 [V Nb Ta] N4	96940	71547	67560	1.26–1.40
LiAlCl4	[Li * K] Ga I4	60850	400816		1.09
	Li Ga [Cl Br I]4	60849	61337	60850	0.82–1.03
LiCs2Cr(CN)6	[Na K Rb] Cs2 Fe C6 N6	411123	411124	411125	1.24–1.69
LiSbF6	Li [P As Sb] F6	74830	74831	23924	0.68–1.12
Metavariscite	[Al * In] H4 P O6	2643	280068		1.41
Mg2SiO4	Mn2 Si [O S Se]4	26376	65710	80957	0.67–0.76
	Mn2 Ge [O S Se Te]4	23587	202054	391296	0.51–0.72
		165681			
MgB4O7	[Zn Cd Hg] B4 O7	424545	14361	281287	0.59–1.46
MgSO3(H2O)6	Mg H12 [S Se Te] O9	48112	48115	48114	0.21–0.49
MgSeO3	[Zn Cd Hg] Se O3	163221	75273	79694	0.89–2.26
Mn2O3	[Be Mg Ca]3 N2	412667	411210	410754	0.64–1.01
MnP	[Cr * W] P	42082	42056		0.63
Na2HgO2	[Na K Rb]2 Hg O2	25511	66275	66276	0.80–1.18
	[Ca Sr Ba]2 Zn N2	69049	80376	80377	0.77–0.89
Na2K3SnP3	Na2 [K * Cs]3 Sn P3	50532	50533		0.81
Na3AsS3	[K Rb Cs]3 Sb Se3	89607	89608	89609	1.27–1.48
	K3 Sb [O * Se Te]3	279579	89607	300182	1.04–1.34
	Rb3 Bi [O * Se]3	407294	85411		1.08
	Cs3 Sb [O * Se]3	279580	89609		1.24
Na3Rh(NO2)6	Na3 [Co Rh Ir] N6 O12	39573	39571	39572	1.50–1.60

Tab. 1 (continued)

Structure type	Series formula			ICSD Coll. Codes	*Q* range
Na5FeO4	K4 Cs [Ga * Tl] O4	48119	74955		1.15
Na6Ge2Se7	Na6 [Si Ge Sn]2 Se7	300236	57089	300235	0.73–1.35
NaCl	[Mg Ca Sr] O	52026	163628	109461	0.63–0.78
	[V Nb Ta] N	22321	982	185287	0.43–0.58
	Pb [S Se Te]	38293	38294	38295	0.72–0.85
	Li Sb [S * Te]2	40456	67505		0.74
	Li [F * * I]	41409	414244		0.85
NaCrS2	Na Er [O S Se]2	97544	73481	50195	0.72–0.76
NaFeO2(beta)	Li [Al Ga In] Se2	280225	96915	60838	0.97
NaLa6OsI12	Sc7 Co [Cl Br I]12	424476	424474	63303	0.72–0.91
NaN3(beta)	[Mg * Sr] C N2	75039	59860		1.09
Ni(NH3)6Cl2	Mn H18 N6 [Cl * I]2	78861	202342		1.55
	Fe H18 N6 [Cl Br I]2	78862	78863	202343	1.29–1.78
Pb2OSO4	Pb2 [Cr * W] O5	710043	61399		1.16
PbCl2	Ba [Cl Br I]2	262674	262675	15707	0.83–1.02
	Pb [F Cl Br]2	161080	202130	202134	0.60–0.77
PbClF/Cu2Sb	Li [Na K Rb] S	61091	47229	67254	0.66–0.98
	[Ca Sr Ba] H Cl	37199	37200	37201	0.97–1.05
	[Ca Sr Ba] Cl F	1130	68373	201514	0.88–0.99
	U [S * Te] O	85845	22204		0.56
	Li K [S * Te]	47229	67887		1.31
	Ba [Cl Br I] F	201514	35393	1128	0.68–0.88
	Pb [Cl * I] F	39165	279599		0.87
PbMo6Cl14	Mo6 Pb [Cl Br I]14	36572	36573	36574	0.73–1.02
PbPS3	[Ca Sr Ba] P Se3	412765	412766	412768	0.94–1.06
Rb2Cl6(NbN3)3H2O	[K Rb Cs]2 Nb3 H2 N9 O Cl6	402487	78833	401705	0.94–1.42
Rb2Pt(CN)4Br2	[K Rb Cs]2 Pt C4 N4 I2	413706	421673	421657	1.37–1.54
	K2 Pt C4 N4 [Cl Br I]2	413704	413705	413706	0.32–0.59
Rb2SiP4O13	H8 [Si * Sn] P4 N2 O13	637	158944		1.58
RbAuS	[K Rb Cs] Au Se	40759	402190	71655	1.13–1.21
Rh(PO3)3	[Al Ga In] P3 O9	170	410180	155165	1.35–1.72
RuCl3(NH3)5	[Co Rh Ir] H15 N5 Cl3	22142	10199	60796	0.92–3.63
Sb2S3	Gd2 [S Se Te]3	33785	99997	68340	0.62–0.84
Sc2S3	Er2 [Se Te]3	79227	50501		0.95
Sn2F6	Na [P As Sb] F6	90615	184564	56251	1.32–1.64
SnI4	[Si Ge Sn] I4	91745	67896	51571	0.44–1.40
Sodalite-frame	Be3 Mn4 Si3 [S Se Te] O12	201638	83839	83840	0.85–1.33
SrCl2H2O	Sr H2 O [Cl Br I]2	60883	37083	60885	0.80–0.95
SrZrS3	[Ca Sr Ba] Zr S3	23286	154104	23288	0.63–0.82
TeBr3AsF6	As [S * Te] Br3 F6	202502	200689		1.15
	As Se [Cl * I]3 F6	66843	202503		0.89
TeSC(NH2)2Cl2	H8 C2 N4 Te S2 [Cl Br I]2	62059	62060	62061	1.09–1.33
ThCr2Si2	[Ca * Ba] Ni2 P2	10461	85408		1.06
TiO2(tP6)	[V Nb Ta] Rh O4	55526	86826	86827	0.87–0.92
	[Mn * Re] O2	393	154021		0.73
	[Si Ge Sn Pb] O2	93549	637460	169032	0.73–1.00
		43460			
TiS3	[Ti Zr Hf] S3	42072	42073	42074	1.29–1.38
TiTe3O8	[Ti Zr Hf] Te3 O8	9076	409713	9078	2.45–2.53
Tl2Ge2S5	[K Rb Cs]2 Ge2 S5	411027	411028	409455	0.98–1.51
Tl2S5	[K Rb Cs]2 S5	44675	100321	201073	1.15–1.28
Tl3AsS4	K3 [V * Ta] S4	81413	59355		2.38
	Cs3 [P As Sb] Se4	415021	404082	404083	1.03–1.49
Tl4UO2(CO3)3	U [K * Cs]4 C3 O11	200698	151876		1.17
Tl6I4S	Tl6 S [Cl Br I]4	35289	40521	29265	0.86–1.03
U3S5	K2 Pr [Cl Br I]5	48190	48191	48192	0.86–1.07

Tab. 1 (continued)

Structure type	Series formula			ICSD Coll. Codes	*Q* range
Variscite	[Al Ga In] H4 P O6	819	86632	80297	0.95–1.13
	[Al Ga In] H4 As O6	170740	407203	94853	0.68–1.06
Zn4B6O13	Sr4 Al6 [S * Te] O12	67590	82609		0.80
ZnBr2	[Zn * Hg] I2	2404	281134		0.66
ZnS(cF8)	[Zn Cd Hg] S	77082	81925	24094	0.37–0.89
	Zn [S Se Te]	77082	77091	104196	0.84–0.89
	Cd [S * Te]	81925	93942		0.98
	Cu [Cl Br I]	78270	78274	78265	0.76–0.77

Series providing for one of the four extreme outliers[2] (outside the 5 σ range) are flagged with "[a]", the extreme outlier values are not accounted for in the corresponding *Q* ranges. Note: A more detailed HSIS Table can be found in the Supplemental Material.

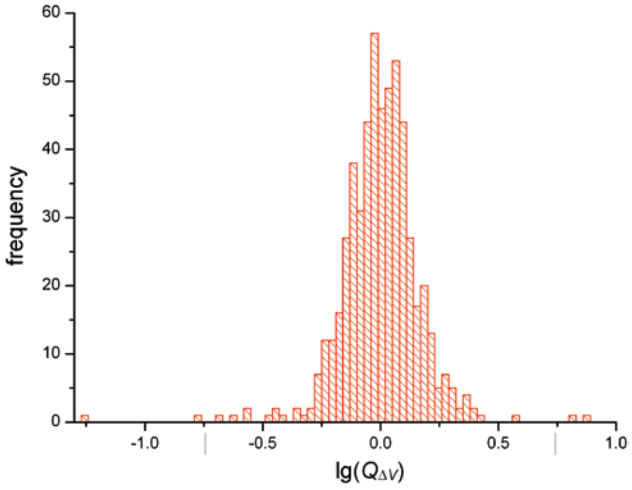

Fig. 5: Distribution of $\lg(Q_{\Delta V})$ values for the 557 data points. The four values differing by more than 5 σ (= 0.74, gray vertical lines) from the mean value are counted as extreme outliers[2] and are not accounted for in the calculation of mean values and standard deviations.

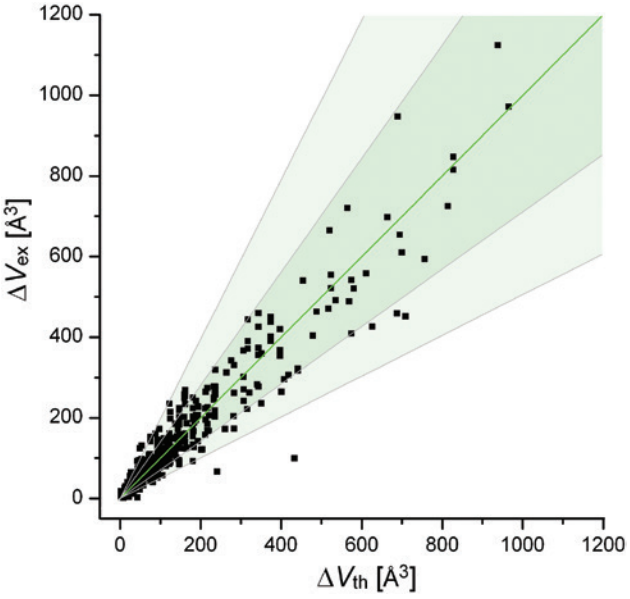

Fig. 6: ΔV_{ex} as a function of ΔV_{th} as calculated by (4). For the central straight line of slope 1, the bent red line and the shaded regions, see text. For an enlarged representation of the range $\Delta V_{th} < 425$ Å³, see Figure 8.

i.e. half the amount expected (0.335 Å), if the expansion model in Figure 2 was valid. Or, to be more exact, a *quarter* of the expected amount, as there are *two* $E(j)$ atoms per unit cell in Figure 7, the "pushing power" of which should add up. Apparently, angular distortions take care for the "volume expansion wave" to flatten when the distance to E increases. As a consequence, $Q_{\Delta V}$ is only 1.04, while for an un-weakened expansion a value of ≈ 4 would result.

At a closer look, such an expansion "wave" (flattening or not) is generally restricted to the "influence domain" of E (in distinction to vicinal E atoms). E.g. in Figure 7 (Figure 2), it must end at the 3rd [4th] coordination sphere where it encounters opposing equivalent waves "sent" from its E neighbors. In most other cases the domain is less extended. E.g. for Figure 1 and, generally, for structures belonging to

Tab. 2: $\langle\lg(Q_{\Delta V})\rangle_E$ for subsets of the HSIS pool with $E(i)$ restricted to a certain element of a certain valence; m is the number of structure pairs contributing to $\langle\lg(Q_{\Delta V})\rangle_E$.

$E(i)$	$\langle\lg(Q_{\Delta V})\rangle_E$	$10^{\langle\lg(Q)\rangle}$	m	$E(i)$	$\langle\lg(Q_{\Delta V})\rangle_E$	$10^{\langle\lg(Q)\rangle}$	m
Na^{+I}	– 0.01(13)	0.98	21	Si^{+IV}	– 0.08(16)	0.83	22
K^{+I}	0.07(10)	1.17	78	Ge^{+IV}	– 0.01(10)	0.98	11
Rb^{+I}	0.06(09)	1.15	30	O^{-II}	– 0.03(12)	0.93	20
Ca^{+II}	– 0.02(10)	0.95	41	S^{-II}	– 0.07(12)	0.83	58
Sr^{+II}	– 0.09(23)	0.81	18	Se^{-II}	– 0.03(15)	0.93	25
Al^{+III}	0.05(13)	1.12	31	Cl^{-I}	–0.04(11)	0.91	59
Ga^{+III}	0.05(12)	1.12	14	Br^{-I}	0.00(10)	1.00	27

2 Two of the four extreme outliers are caused by Rh → Ir transitions [$\Delta\rho = 0.01(1)$ Å], and one by Cd → Hg (0.05(3) Å). The fourth one, with $Q_{\Delta V} = 0.06$, implies an $Sb^{+III} \rightarrow Bi^{+III}$ transition [$\Delta\rho = 0.13(4)$ Å], it is therefore probably mainly due to the shrinking lone-pair electron. In all four cases, ΔV_{ex} is < 18 Å³.

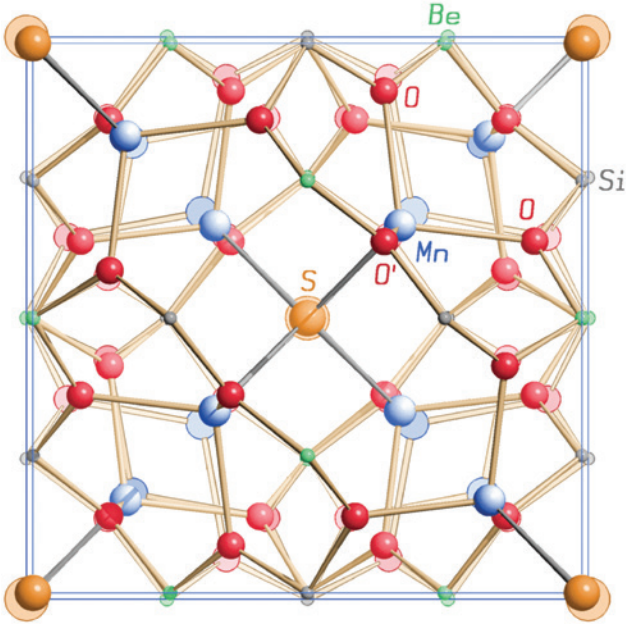

Fig. 7: Superimposition of the structures of the two end members of the series $Be_3Mn_4Si_3[S\ Se\ Te]O_{12}$. The S [Te] structure has been visualized by solid 3D [flat] shading. The four bond sticks in the center connect the central S [Te] atom (orange) to four Mn atoms (blue).

simple structure types like ZnS or NaCl the "wave" must already end in reaching the 1st coordination sphere.

Extended domains like in HS-1 can only exist if the E concentration is low. E.g. for HS-1, c_E is 0.0036 Å^{-3}, to be compared to 0.0253 Å^{-3} for Zn[S Te]. Therefore the question of wave flattening can arise only for HSIS with a small c_E. Apparently, not all the corresponding structures manage things as well as HS-1 ($0.85 \le Q_{\Delta V} \le 1.33$): for all transitions in the HSIS of Table 1 which generate $Q_{\Delta V}$ values > 1.7, c_E is ≤ 0.007 Å^{-3}. Prominent examples are the transitions to Ba in $K_2[Ca\ Sr\ Ba]CuN_6\ O_{12}$ ("HS-2") (STT: $K_2SrCu_2(NO_2)_6$) with $Q_{\Delta V} = 1.88$ and $2.18/c_E = 0.0035$ Å^{-3} and $[K\ Rb\ Cs]RuH_{18}N_6O_8Cl_4$ ("HS-3") (STT: $KOs(NH_3)_6\ (ClO_4)_2Cl_2$) with $1.94 \le Q_{\Delta V} \le 2.11/c_E = 0.0025$ Å^{-3}. In both cases, E is surrounded by polyatomic ions, within (and partially even beyond) which the atomic expansion shifts are passed on rather constantly (i.e. with no or only slight "wave" flattening). The above $Q_{\Delta V}$ values would therefore even be larger, if not the *initial* shifts (1st coordination sphere) were already significantly smaller than expected: 0.21 Å instead of 0.34 [0.28] Å in HS-2 (Ca → Ba) [HS-3 (K → Cs)]. We do not go so far to claim, though, that these reductions are induced by the desire to keep $Q_{\Delta V}$ as close to 1 as possible.

Low c_E values can, on the other hand, also come with *low* $Q_{\Delta V}$ values. A pronounced, though certainly not typical, example is $Cs_3[Cr\ Mo]_2Cl_9$ (STT: $Cs_3Cr_2Cl_9$) with $c_E = 0.0050$ Å^{-3} and $Q_{\Delta V} = 0.27$. The (special) reason here is, that the E–E distance in the $E_2Cl_9^{3-}$ ion shrinks from 3.17 (E = Cr) to 2.64 Å at practically constant E–Cl(bridge) distances (while those for the terminal Cl ligands grow as expected). Thus, it's probably an increasing bonding E–E interaction which makes $Q_{\Delta V}$ low.

Let's finally go back to (2) once more which suggested that ΔV is dependent from the initial volume $V(i)$. (2) certainly describes relationships correctly as long as we stay within a group of HSIS which all belong to the CsCl structure type. Or to any other cubic structure type, if t and Δr are modified correspondingly (the latter in case of $z_E > 1$). E. g., within the series $[Be\ Mg\ Ca]_3N_2$ with E-N bonds approx. parallel to <111> (see below), (2) predicts ΔV_{ex} with maximally 5% deviation, if t is kept at $2/\sqrt{3}$ and Δr is replaced by $4\ \Delta d_{E(i)\ E(j)}$, where $\Delta d_{E(i)\ E(j)}$ are the differences of the (averaged) E-N bond lengths.

But, across a large number of randomly selected HSIS belonging to various different structure types the dependence from $V(i)$ vanishes, as stated above (see also next section).

Comparison with results derivable from Biltz' volume increments rule

Owing to the hint of an anonymous referee, the results of the above statistical analysis will now be compared to those obtainable when taking Biltz' volume increments rule [13] (of which the author had not been aware before) as a starting point. The rule, published in the 1930s, can be briefly summarized as follows: the molar volume v_m of any compound can be estimated as a sum of increments contributed by the different components of the compound's sum formula according to (7)

$$v_m \approx \Sigma^k \mu(k)\, I(k) \qquad (7)$$

where $I(k)$ is an "incremental" molar volume specific for the k^{th} element in the sum formula and $\mu(k)$ is the stoechiometric coefficient of this element. Biltz [13] and others have statistically determined I values for most elements in their roles as components of ionic compounds. Generally, the I value of an element depends on its valence ς and (more or less) on the chemical context. E.g. in binary phosphides M_mP_p, $I(P^{-III}) = 34$ cm³/mol if the valence of M is + I, and 19 cm³/mole if the valence is + IV [14] while $I(P^{+III}) = 6$ cm³/mol [13]. It has been shown comparatively recently, that I values are related to atomic volumes as determinable by quantum-mechanical methods [15].

Tab. 3: Selected parameters[a] for some HSIS from Table 1.

HSIS	Structure type	ς_E	z_E	$\Delta I_{E(i)\,E(j)}$	$32.8\,\Delta\rho_{E(i)\,E(j)}$	$Q'_{\Delta V}$	$Q_{\Delta V}$
$Be_3Mn_4Si_3$[S Se Te]O_{12}	sodalite-frame	– II	2	3, 8	4.3, 6.9	0.76–1.94	0.85–1.33
Sr H_2O [Cl Br I]$_2$	$SrCl_2H_2O$	– I	8	5, 9	4.9, 7.2	0.77–0.80	0.80–0.95
[Na K Rb Cs]BO_2	KBO_2	+ I	18	9.5, 4, 6	10.8, 3.6, 5.6	0.85–1.05	0.79–1.18
K_2[Ca Sr Ba]CuN_6O_{12}	$K_2SrCu_2(NO_2)_6$[b]	+ II	4	4.5, 5	4.9, 6.2	1.64–2.79	1.45–2.18
[B Al Ga]PO_4	$AlPO_4$	+ III	3	0.5,1.5	9.8, 2.0	5.9–24.4	0.98–1.22
$CoCu_2$[Si Ge Sn]S_4	Cu_2FeSnS_4	+ IV	2	1, 1	3.6, 5.6	2.9–5.6	0.77–0.97
Na[P As Sb]F_6	Sn_2F_6	+ V	4	0, 0	4.9, 5.6	∞	1.32–1.64
Li_2[Cr Mo W]O_4	Be_2SiO_4	+ VI	18	0, 0	3.9, 0.3	∞	0.90–1.04

[a] *I* values tabulated by Biltz [Ref. 13, page 239] have been used. In the case of $\varsigma_E < 0$, they apparently have been determined mainly from cases with counterions of valence + I, while in the two corresponding HSIS the counterions are of valence + II. While *I* values in the latter case should be somewhat smaller, *I differences* (i.e. ΔI values) are supposed to be quite similar.
[b] Stoichiometric factor of Cu is inconsistent.

Now, in a *crystalline* compound, the unit cell volume V_{uc} is related to the molar volume v_m by (8) (with Z = number of formula units per unit cell and A = Avogadro number)

$$V_{uc} = Z\,v_m / A\,[\mathrm{cm}^3] = Z\,v_m\,10^{24} / A = 1.66\,Z\,v_m\,[\mathrm{Å}^3] \qquad (8)$$

Let's now consider two isotypic (and therefore *chemically very similar*) structures with only one element E different in the sum formulas. In estimating the unit cell volume difference $\Delta V'_{th} = 1.66\,Z\,(v_m(j) - v_m(i))$ [Å^3] the identical contributions due to (7) of all elements except $E(j)/E(i)$ vanish and we obtain (9)

$$\Delta V'_{th} = 1.66\,Z\,(\mu_{E(j)} I_{E(j)} - \mu_{E(i)} I_{E(i)}) = 1.66\,z_E\,(I_{E(j)} - I_{E(i)}) = 1.66\,z_E\,\Delta I_{E(i)\,E(j)} \qquad (9)$$

(with $Z\mu_{E(j)} = Z\mu_{E(i)} = z_E$). Thus, the above *qualitative* finding that ΔV for two isotypic structures is supposed to depend – per average – only on z_E and an $E(i)/E(j)$ size difference parameter (and not from $V(i)$) could have been predicted beforehand from the increments rule.

Quantitatively, in the case of the above $Be_3Mn_4Si_3$[S Te]O_{12} example, we obtain from (9) $\Delta V'_{th} = 36.5$ Å$^3 \rightarrow Q'_{\Delta V}$ (= $\Delta V_{ex}/\Delta V'_{th}$) = 1.08, in good agreement with $Q_{\Delta V} = 1.04$. $Q'_{\Delta V}$ and $Q_{\Delta V}$ ranges for the complete series (including the Se structure) and for some other, arbitrarily selected HSIS, each representing another E valence, ς_E, are shown in Table 3. While the two Q ranges are similar for the series with $-\mathrm{II} \le \varsigma_E \le +\mathrm{II}$, we (*systematically*) get bad $Q'_{\Delta V}$ values for $\varsigma_E > +\mathrm{II}$, because many of the corresponding ions (and even the pair Be^{+II}/Mg^{+II}) have been assigned small similar *I* values, some of them all zero across whole periodic table groups. Obviously, (9) cannot be used generally for the estimation of ΔV. We therefore refrained from a statistical analysis of the equation.

Equating (9) and (4) (the latter approximating (6), see above) yields the relation $\Delta I = 32.8\,\Delta\rho$. Corresponding values calculated from $\Delta\rho_{E(i)\,E(j)}$ values [10] (for "vicinal" elements) are shown in Table 3 for comparison. Note that if they were used to redefine *I* for $\varsigma_E > +\mathrm{II}$, this would lead to systematic violations of (7).

Series of structures with an infinite HVAPS-*E* framework

As already mentioned above, some series had been excluded *a priori* from the statistical analysis visualized in Figure 6 due to a non-formal criterion. The reason for this measure was some earlier experience with the series KBi_6O_9[Cl Br I] [5], within which the lengths of the bonds formed by E (and therefore ΔV_{ex}) grow significantly less than expected from $\Delta\rho_{E(i)\,E(j)}$ values. An explanation found was that the "natural" volume expansion caused by $X(i) \rightarrow X(j)$ replacement (X = halogen) is hampered by the rigidity of the infinite framework of dimensionality three formed by the Bi and O atoms: The low valence bonds to $X(j)$ are assumedly too weak to push through its desire to gain more volume against the forces established by the strong high-valence bonds of the Bi-O framework[3] [5].

As KBi_6O_9[Cl Br I] and related series were therefore suspected to systematically produce "too small" ΔV_{ex} values they were tried to be identified in order to

3 A recent closer look showed that things probably are the other way around in this case: bond valence sums calculated by softBV [16] from the KBi_6O_9X structures for the Cl (0.52), Br (0.71), I (1.03) [and K (0.94 – 0.97 v.u.)] atoms suggest that the volume requirements for I [and K] are actually satisfied while the smaller X atoms do not succeed in *shrinking* the Bi-O framework as required for their optimal accommodation – with same downsizing effect on Δa and ΔV_{ex} values.

Tab. 4: HSIS with an infinite HVAPS-*E* of dimensionality $D_H = 1–3$.

Structure type	Series formula			ICSD Coll. Codes	*Q* range
(a) $D_H = 1$					
K2B2S7	[Na * Rb]2 B2 Se7	401098	411469		0.98
K2CuNbSe4	[K Rb Cs]2 Ta Ag S4	84294	84295	84296	1.19–1.29
K2MnS2	[K Rb Cs]2 Mn Te2	65459	65460	65461	1.09–1.15
	[Na K Rb Cs]2 Co S2	67386	67387	67388	0.64–1.16
		67389			
K2Mo3O10	[K Rb Cs]2 Mo3 O10	24118	48213	280066	1.38–1.46
K3Ta2Se2(Se2)3AsSe3	[K Rb Cs]3 Nb2 As Se11	413597	413598	413599	1.19–1.27
Na3Fe2S4	[Na K Rb]3 Fe2 Se4	402274	89587	409454	0.80–1.10
NaBiO2	[Na K Rb Cs] Bi O2	173624	407209	407208	0.74–1.34
		406564			
NaCu2OH(SO4)2H2O	[Na K Rb] Cu2 H3 S2 O10	73265	65784	73266	0.57–3.84
Tl2Se2	In [Na K Rb] Te2	25346	73410	75346	0.49–1.33
(b) $D_H = 2$					
Bi2ErO4I	Y Bi2 O4 [Cl Br I]	92405	92418	92432	0.60–0.67
Ca2CuCl2O2	Sr2 Cu O2 [Cl * I]2	67067	55710		0.93
Cs2Nb3O5Cl7	[K Rb Cs]2 Nb3 O5 Cl7	417791	417793	417790	0.37–1.05
Cu4KS3	[K * Cs] Cu4 S3	23336	23325		0.78
Cu8Rb3Se6	[K Rb Cs]3 Cu8 Se6	85728	14011	14012	0.86–0.87
K2(UO2)2WO6	[K Rb Cs]2 U2 W O10	96441	96442	160302	0.71–1.05
K2Al2Sb3	[Na K Rb]2 In2 Sb3	300192	71245	83663	0.79–1.11
K2Co3(OH)2(SO4)3(H2O)2	[K * Cs]2 Cd3 H6 S3 O16	201165	201164		1.02
K2Pt4Se6	[K Rb Cs] Pt2 Se3	69438	69439	69440	0.97–1.01
K2UO2(MoO4)2H2O	[K Rb Cs]2 U Mo2 H2 O11	94734	92597	171032	0.65–1.15
K4Ta4P4S24	[K Rb Cs] Ta P S6	59915	412970	170287	1.00–1.28
KInS2	[K Rb Cs] In S2	300153	415554	415553	0.89–0.98
KPbPS4	[K Rb Cs] Pb P S4	171379	249870	409821	0.76–0.86
KUO2VO4	[Na * * Cs] U V O6	423817	66389		0.82
Na2YMoO4PO4	[K * Cs]2 W Bi P O8	249162	260559		0.82
PbClF/Cu2Sb	U [S Se Te] As	66945	66946	42353	0.81–0.83
	Bi O [F Cl Br I]	201620	74502	61225	0.44–0.86
		391354			
Rb3Cu5O4	[K Rb Cs]3 Cu5 O4	94387	35246	94388	0.74–1.25
SmSI	Zr N [Cl Br I]	93740	51771	51772	0.49–0.54
	Hf N [Cl Br I]	93741	51773	51774	0.47–0.53
(c) $D_H = 3$					
Boracite	Mn3 B7 O13 [Cl Br I]	402906	402907	402908	0.13–0.20
Boracite(HT)	Cr3 B7 O13 [Cl Br I]	4231	66352	62178	0.14–0.28
Ca5(PO4)3Cl	Pb5 P3 O12 [F Cl Br]	166321	203075	181837	0.61–0.68
Ca9MgNa(PO4)7	[Na K * Cs] Ca10 P7 O28	91524	91525	380395	0.18–0.54
CaB2O4(HP)	[Na K Rb] Ga Sn S4	417380	417381	417382	0.08–0.87
Cr5CsS8	[K Rb Cs] Cr5 S8	2568	2567	2566	0.47–0.47
Cu3Bi(SeO3)2O2Cl	Cu3 Bi Se2 O8 [Cl Br I]	54190	280759	54191	0.47–0.51
In2Mo15Se19	[K Rb Cs]2 Mo15 S19	280948	91321	59830	0.60–0.67
K(MoO)5(P2O7)4	[Li Na K] Mo5 P8 O33	417727	417728	417726	0.32–0.41
K2GeTeO6	[K Rb Cs]2 Ge Te O6	40422	40423	40424	0.09–0.13
K2Mg2(SO4)3	[Na K * Cs] Ba In2 P3 O12	96059	96060	96061	0.39–0.53
K2SrCu2(NO2)6	[K Rb Cs]2 Cu Pb N6 O12	1274	372	56252	0.58–0.83
K2TiSi6O15	[K Rb Cs]2 Ti Si6 O15	93569	93568	89988	0.80–0.83
K3P6Ni11	[K Rb Cs]3 P6 N11	50211	51396	51397	0.46–0.49
KAlO2	[K Rb Cs] Fe O2	421185	421187	421189	0.71–0.74
KAlP2O7	[K Rb Cs] Y P2 O7	160190	72468	74599	0.72–0.85
KAlSi3O8	[Na K Rb] Al Si3 O8	88898	10270	9102	0.58–0.65
KAs4O6Br	K As4 O6 [Cl Br I]	65205	65206	65207	0.26–0.58
KBi6IO9	K Bi6 O9 [Cl Br I]	408653	408654	408652	0.45–0.64
KGd(PO3)4	[K Rb Cs] Eu P4 O12	260599	167790	260554	0.39–0.55

Tab. 4 (continued)

Structure type	Series formula			ICSD Coll. Codes	*Q* range
KMoO2PO4	[K * Cs] Mo P O6	86442	411703		0.43
KNi(H2O)2Al2(PO4)3	[K * Cs] Mn Ga2 H4 P3 O14	261118	710069		0.31
KTh2(VO4)3	[K Rb Cs] Th2 P3 O12	30432	154632	154633	0.44–0.46
KTiPO5	[K Rb Cs] Ti As O5	75322	170751	65675	0.44–0.48
La3(SiO4)2Cl	Pr3 Si2 S8 [Cl Br I]	412223	411998	411781	0.31–0.50
LiNbWO6H2O	[Li * K] Nb W H2 O7	4143	18065		0.11
Na2Re3S6	[Na K Rb]2 Re3 S6	200835	200836	79583	0.53–1.01
NaZr2(PO4)3	[Li Na K Rb] Ti2 P3 O12	95979	20776	67091	0.04–0.56
		75235			
PbCl2[a]	Bi S [Cl Br I]	100173	31389	23631	0.49–0.73
	Bi Se [Cl * I]	40862	280311		0.87
Rb2Ge4O9	[Na K Rb]2 Ge4 O9	51106	31969	91	0.54–0.77
Sodalite-frame	Na4 Al3 Ge3 O12 [Cl Br I]	65664	65665	65666	0.75–0.82
TlNbTeO6	[K Rb Cs] W Sb O6	181570	9526	165063	0.05–0.18

[a]Secondary Bi–S [Bi–Se] bonds counted as framework bonds, otherwise D_H would be 1.

exclude them from the statistical analysis. To this end, the structures for which the (absolute) valence of *E*, $|\varsigma_E|$, is I or II were inspected not only to check for isotypism but also with respect to what might be called their "higher valence atoms partial structure with respect to *E*" (HVAPS-*E*). The latter is obtained by removing from the structure all atoms *E* plus all other ions with the *same* or a *lower* (absolute) valence. For example, to get the HVAPS-B in $NaBSiO_4$, all B, Na and O atoms have to be removed, thus the HVAPS-B consists only of the remaining isolated Si atoms. With this definition of the HVAPS-*E*, the criterion for exclusion was that the latter forms an infinite framework of dimensionality 1, 2 or 3. The idea behind is, that the valences (i.e. strengths) of bonds formed by an atom sum up to the valence of this atom [17]. On the (occasionally simplifying) assumption that the coordination numbers of all atoms in the structure are at least similar, the HVAPS-*E* correspondingly should contain only bonds (if any) which are strong as compared to the bonds formed by *E*. Therefore, if the HVAPS-*E* is an infinite framework, its bonds should be able to offer resistance to attempts of the weak *E* bonds to expand or shrink the structure (but not, if the HVAPS-*E* consists of isolated atoms or building blocks).

Exclusion of HSIS according to the above criterion involved mainly series with *E* = alkali/halogen as it turned out to be unlikely that the HVAPS–*E* in the case of $|\varsigma_E| > I$ contain infinite frameworks. One counter example, UAs[S Se Te], can be found in section (b) of Table 4.

While the series found to match the criterion did not contribute to the calculations described above, they were looked at more thoroughly at a later stage. To this end, $Q_{\Delta V}$ values were calculated by means of (6) for the subsets of series with equal dimensionality D_H of the HVAPS-*E* framework (Table 4).

Table 5 shows $<\lg(Q_{\Delta V})>$ values and standard deviations for the different groups of constant D_H. Values for $D_H = 0$ refer to the pool which was used for the statistical analysis (above). It is obvious, that the $<\lg(Q_{\Delta V})>$ values become "worse" (i.e. more negative) the higher D_H. In the case of $D_H = 3$, $<\lg(Q_{\Delta V})>$ is approx. 2.5 σ (as calculated for $D_H = 0$) lower than 0.000. This shows that in many of the corresponding HSIS, *E*(*j*) [*E*(*i*)] is not capable to put through its desire for more [less[3]] space against the HVAPS framework when it replaces *E*(*i*) [*E*(*j*)]. The effect is much smaller for $D_H = 2$, and not recognizable any more for structures with $D_H = 1$.

In Figure 8, a ΔV_{ex} vs. ΔV_{th} diagram is shown for the two groups of series with $D_H = 0$ and 3. All ΔV_{ex} [ΔV_{th}] values of the latter are < 250 [350] A^3 and all corresponding data points (drawn with light color) except one[4] are below

Tab. 5: $<\lg(Q_{\Delta V})>$ values for HSIS sets of different HVAPS-*E* framework D_H values. m_{STT} = number of structure types, m_{ser} = number of series, m_{pairs} = number of data points.

D_H	m_{STT}	m_{ser}	m_{pairs}	$<\lg(Q_{\Delta V})>$	$10^{<\lg(Q)>}$
0	170	228	553	0.000(148)[a]	1.00
1	9	10	34	0.028(156)	1.07
2	18	20	53	– 0.100(120)	0.81
3	32	33	94	– 0.377(283)[b]	0.42

[a]Four extreme outliers (outside the 5σ range) excluded; [b]No outliers excluded; values are distributed very asymmetrically between –1.4 and 0.0.

4 $Q_{\Delta V} = 1.01$ for the K→Rb transition in $[Na\ K\ Rb]_2Re_3S_6$ (STT: $Na_2Re_3S_6$) where the HVAPS-*E* consists of Re_6S_8-clusters comparatively wide-meshedly connected via (di-) sulfide bridges.

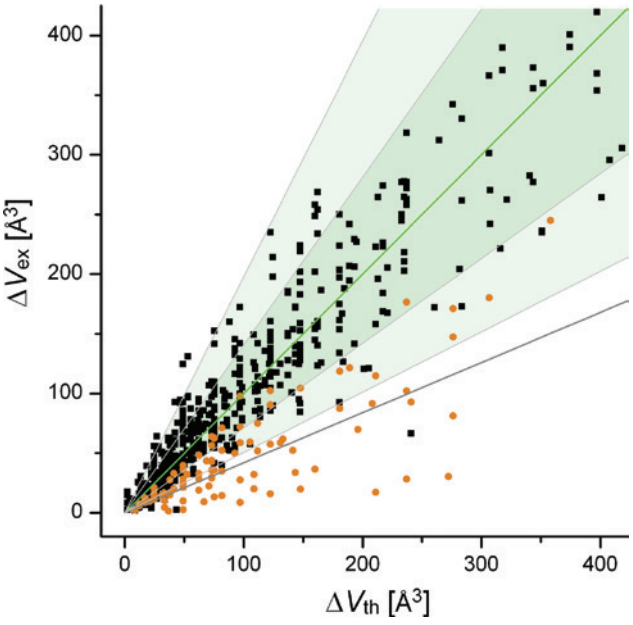

Fig. 8: ΔV_{ex} as a function of ΔV_{th} for HSIS with an HVAPS-*E* framework of dimensionality 0 (black square-shaped spots, cf. Figure 6) and three (circular spots drawn with lighter color). The (gray) straight line representing $10^{<\lg(Q)>} = 0.42$ (Table 5, $D_H = 3$) runs below the 2σ range (shaded area) of the data point distribution for $D_H = 0$. Shaded areas visualize 1σ and 2σ regions of $<\lg(Q_{\Delta V})>$.

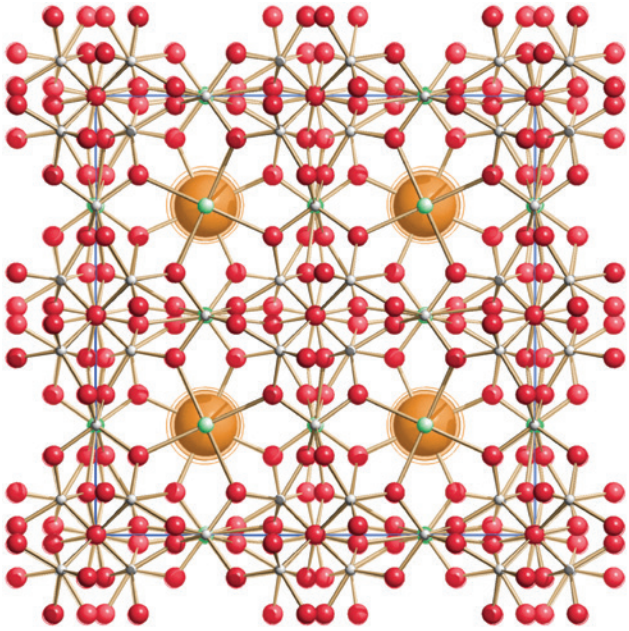

Fig. 9: Superimposition of the three structures of the series $Cr_3B_7O_{13}$[Cl Br I] with $D_H = 3$. Halogen atoms (large spheres) have been drawn with orange color. Bond sticks to the halogen atoms have been omitted (the four sticks seemingly connecting the halogen atoms with surrounding O atoms, actually belong to a Cr atom in the background). The $Q_{\Delta V}$ values for this HSIS are in the range 0.14–0.28.

the slope 1 line. In contrast, the data points for series with $D_H = 1$ and 2, if included, would mingle (almost) undistinguishably with those of $D_H = 0$.

Because of the cases with $D_H = 3$, (6) should not be applied without knowledge of the $E(i)$ crystal structure, if $|\varsigma_E| = I$, except when the sum formula shows that the HVAPS-*E* consists of isolated atoms (as in the $NaBSiO_4$ example above).

In Figure 9, a pronounced example of a series with $D_H = 3$ and $z_E = 8$ is shown, the series $Cr_3B_7O_{13}$[Cl Br I] (STT: Boracite (HT); Table 4c). That three crystal structures are superimposed here, can practically only be seen from the nearly concentric circles (indicating Br and I) around the Cl atoms (all halogen atoms drawn with orange color). As a contrast, the above mentioned series $[Be\ Mg\ Ca]_3N_2$ (STT: Mn_2O_3; Table 1) with $z_E = 48$, $D_H = 0$ is shown in Figure 10.

Although usually $Q_{\Delta V}$ values comparatively close to 1 are obtained for $D_H = 1$ or 2, the corresponding HVAPS-*E* frameworks can nevertheless show the expected rigidity. This is, however, restricted to one or two dimensions, while the remaining dimension(s) can be used for compensation. Therefore often a significant anisotropy of the unit cell expansion can be observed in such cases: If $D_H = 1$ and the framework rods run parallel to one of

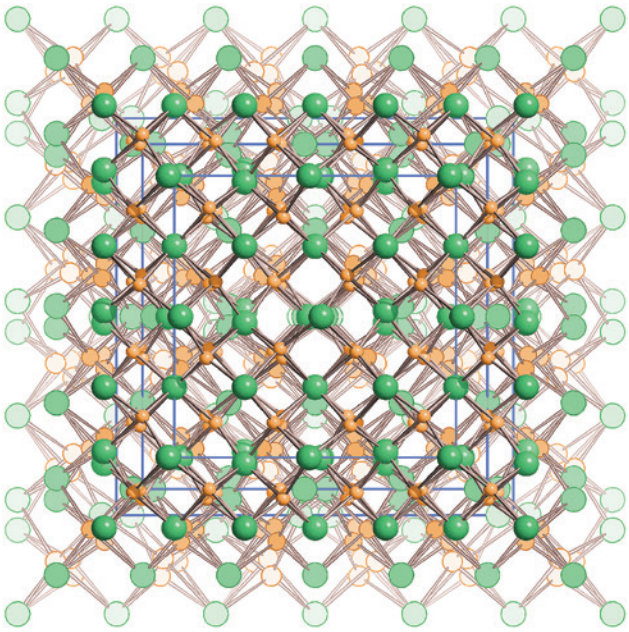

Fig. 10: Superimposition of the three structures of the series $[Be\ Mg\ Ca]_3N_2$ with $D_H = 3$. Parallel (!) projections of structures have been visualized by solid 3D shading (Be structure), strong (Mg) and weak (Ca) flat shading. N atoms (largest spheres) have been drawn with green color. The $Q_{\Delta V}$ values for this HSIS are in the range 0.64–1.01.

Tab. 6: Lattice parameter changes, Δa, Δb, Δc [Å] for "vicinal" structures in HSIS with $D_H = 1$ or 2 (cf. Table 4).

Series	STT	D_H	Orient.[a]	Δa[b]	Δb	Δc	$Q_{\Delta V}$
[Na K Rb Cs] BiO_2	$NaBiO_2$	1	[001]	0.52	0.58	*0.09*	0.75
				0.23	0.48	*0.01*	1.34
				0.21	0.82	*0.00*	1.25
[Na K Rb] $InTe_2$	Tl_2Se_2	1	[001]	0.27	0.27	*0.04*	0.49
				0.22	0.22	*0.06*	1.33
$[K\ Rb\ Cs]_2\ TaAgS_4$	$K_2CuNbSe_4$	1	[100]	*0.02*	0.36	0.85	1.29
				0.02	0.84	1.11	1.19
[K Rb Cs] Pt_2Se_3	$K_2Pt_4Se_6$	2	(001)	*– 0.01*	*– 0.01*	0.80	0.97
				0.01	*0.01*	1.16	1.01
Zr N [Cl Br I]	SmSI	2	(001)	*0.04*	*0.04*	1.60	0.49
				0.08	*0.08*	2.11	0.54
[Na * * Cs] UVO_6	KUO_2VO_4	2	(100)	1.29	*0.10*	*0.10*	0.82

[a]Orientation of the HVAPS-*E* framework rods or layers. [b]Unusually small changes in lattice parameters are printed in italic.

the unit cell axes, the corresponding lattice parameter is usually the one to change least. Similarly, if $D_H = 2$ and the framework layers run parallel to one of the unit cell faces, the corresponding two lattice parameters are the ones to change least. Pronounced examples are given in Table 6.

Conclusions

Due to a statistical analysis of the unit cell volume increase ΔV in 228 homogeneous series of isotypic structures (HSIS) of "ionic" compounds with varying element $E(i)$ the "expectation value" ΔV_{th} can be expressed as a 2nd order function of the product of $\Delta\rho$ (the linear size increase of $E(i)$) and z_E (the number of E atoms per unit cell), as given by (6). Other than anticipated by the author from (2), ΔV_{th} is independent from the initial volume $V(i)$, a result which could have been derived beforehand from Biltz' volume increments rule [13].

There are cases where (6) is not applicable: for an E of valence ±1, ΔV is, with considerably high probability, severely over-estimated by (6), if the "higher valence atoms partial structure with respect to E" (HVAPS-E) of the corresponding HSIS forms an infinite framework of dimensionality 3. Aside from these (comparatively few) exceptions, any observed ΔV_{ex} value is supposed to be in the range one half to twice the value calculated by (6). While (6) correspondingly predicts an *unknown* ΔV with rather high uncertainty it should – at least – allow, on the other hand, to classify any *known* ΔV_{ex} value as "(very) low", "quite normal", or "(very) high", depending on which one of the differently coloured regions of Figure 6 (including the two white ones) would be occupied by the corresponding ΔV_{ex} vs. ΔV_{th} data point.

The principal compatibility of our findings with the volume increments rule suggests that the results presented here are not restricted to HSIS of ionic compounds but can – in principle – be transferred to all isotypic series of compounds where only one element E in the sum formula is exchanged by another one, at least, if $\Delta\rho$ is, where appropriate, replaced by a more suitable value like, e.g., the metal radii difference.

Acknowledgements: The author thanks Dr. S. Rühl of the FIZ Karlsruhe, Germany, for providing him with a "light" version of the ICSD in ASCII format. He is also indebted to an anonymous referee for his/her hint regarding Biltz' "raumchemische" investigations. Financial support by the "Deutsche Forschungsgemeinschaft" regarding the development of FINDIS (KE 793/4-1) is gratefully acknowledged.

References

[1] J. Lima-De-Faria, E. Hellner, F. Liebau, E. Makovicki, E. Parthé, Nomenclature or inorganic structure types. *Acta Cryst.* **1990**, *A46*, 1.

[2] G. Bergerhoff, R. Hundt, R. Sievers, I. D. Brown, The inorganic crystal structure data base. *J. Chem. Inf. Comput. Sci.* **1983**, *23*, 66.

[3] FIZ Karlsruhe, Inorganic Crystal Structure Database (ICSD), **2016**, http://icsdweb.fiz-karlsruhe.de.

[4] R. Allmann, R. Hinek, The introduction of structure types into the Inorganic Crystal structure Database ICSD. *Acta Cryst.* **2007**, *A63*, 412.

[5] E. Keller, V. Krämer, Experimental versus expected halide-ion size differences; structural changes in three series of isotypic bismuth chalcogenide halides. *Acta Cryst.* **2006**, *B62*, 417.

[6] E. Keller, C. Röhr, Structural changes within and between the two isotypic series $ABiO_2$ (A = Na, K, Rb, Cs) and $ASbO_2$ (A = K, Rb, Cs). *Z. Kristallogr.* **2008**, *223*, 431.
[7] P. Schultz, E. Keller, Strong positive and negative deviations from Vegard's rule: X-ray powder investigations of the three quasi-binary phase systems $BiSX_{1-x}Y_x$(X, Y = Cl, Br, I). *Acta Cryst.* **2014**, *B70*, 372.
[8] E. Keller, Extraktion homogener isotyper Strukturserien aus der ICSD. *Z. Kristallogr. Suppl.* **2009**, *29*, 24.
[9] S. Rühl, FIZ Karlsruhe, Germany, **2013**, personal communication.
[10] E. Keller, V. Krämer, 'Ionic' size differences from bond-valence parameters and from ionic radii. *Acta Cryst.* **2006**, *B62*, 411.
[11] E. Keller, SCHAKAL 99. Universität Freiburg, Germany, **2004**.
[12] Origin Lab Corporation, *Origin*, version 7.0303. Northampton, MA, USA, **2002**.
[13] W. Biltz, Raumchemie der festen Stoffe. L. Voss, Leipzig, **1934.**
[14] W. Klemm, H.-G. v. Schnering, Die molaren Volumina von Metall-Phosphiden. *Z. Anorg. Allg. Chem*. **1982**, *491*, 9.
[15] A. Baranov, M. Kohout, F. R. Wagner, Y. Grin, R. Kniep, W. Bronger, On the volume chemistry of solid compounds: the legacy of Wilhelm Biltz, *Z. Anorg. Allg. Chem.* **2008**, *634*, 2747.
[16] S. Adams, softBV. Universität Göttingen, Germany, **2004**, http://www.softbv.net.
[17] I. D. Brown, Chemical and steric constraints in inorganic solids. *Acta Cryst.* **1992**, *B48*, 553.

Supplemental Material: The online version of this article (DOI: 10.1515/zkri-2016-0005) offers supplementary material, available to authorized users.